10^{-5} to 10^{-6} m/sec. This effect cannot be resolved from the Pioneer 11 tracking data.

If the mean time between penetrating impacts was 24 to 120 seconds for the entire 1100-second passage through the E ring, only 9 to 46 of the 147 active cells would have been penetrated during the first crossing. That would leave many cells remaining for the flight under the rings and for the second E ring crossing. A similar loss of cells would be expected during the second E ring crossing. Unfortunately, both channels were inhibited for most, or all, of the second E ring crossing as the result of impacts that occurred while the spacecraft was beneath the bright rings of Saturn. These last impacts were probably from particles ejected from the optically thick rings as the result of collisions between ring particles or between meteoroids and ring particles.

D. H. HUMES, R. L. O'NEAL
W. H. KINARD, J. M. ALVAREZ
NASA/Langley Research Center, Hampton, Virginia 23365

References

1. D. H. Humes, J. M. Alvarez, W. H. Kinard, R. L. O'Neal, *Science* **188**, 473 (1975).
2. R. L. O'Neal, *NASA Tech. Note D-7691* (1974).
3. D. H. Humes, in *Jupiter*, T. Gehrels, Ed. (Univ. of Arizona Press, Tucson, 1976), p. 1052.
4. J. M. Alvarez, *NASA Tech. Note D-4284* (1968).

3 December 1979

The Magnetic Field of Saturn: Pioneer 11 Observations

Abstract. *The intrinsic magnetic field of Saturn measured by the high-field fluxgate magnetometer is much weaker than expected. An analysis of preliminary data combined with the preliminary trajectory yield a model for the main planetary field which is a simple centered dipole of moment 0.20 ± 0.01 gauss-R_S^3 = 4.3 ± 0.2 × 10^{28} gauss-cm^3 (1 R_S = 1 Saturn radius = 60,000 km). The polarity is opposite that of Earth, and, surprisingly, the tilt is small, within 2° ± 1° of the rotation axis. The equatorial field intensity at the cloud tops is 0.2 gauss, and the polar intensity is 0.56 gauss. The unique moon Titan is expected to be located within the magnetosheath of Saturn or the interplanetary medium about 50 percent of the time because the average subsolar point distance to the magnetosphere is estimated to be 20 R_S, the orbital distance to Titan.*

The Pioneer 11 high-field fluxgate magnetometer (FGM) experiment (*1*) consists of two biaxial fluxgate sensor assemblies and an associated electronics system; it is designed to measure fields up to 10 gauss along three orthogonal axes. This ultralightweight instrument, having low power requirements and a low bit rate, was selected for addition to the spacecraft only 3 months before launching in April 1973, in order to provide a higher upper range than that provided by the helium vector magnetometer, whose maximum measurable field is 1.4 gauss (*2*). Spin-synchronous, instantaneous vector measurements were obtained by the FGM at approximately 144-second intervals at Saturn, the sampling rate being determined by the spacecraft's spin period (7.7 seconds) and telemetry rate (0.2 bit per second) allocated to this experiment. The instrument response characteristics, coupled with the use of 10-bit analog-to-digital converters, yield a quantization step size of ± 600 γ (1 $\gamma = 10^{-5}$ gauss) for measured fields of intensity less than 2 gauss. The total weight of the instrument is 272 g, and the power required, 300 mW, was supplied by the cosmic-ray telescope experiment.

The results presented here are based on preliminary experiment data records and preliminary spacecraft trajectory and inertial attitude information. The clock or phase angle of the sun as seen from the spacecraft is extremely sensitive to errors in attitude determination since the spacecraft spin axis is directed toward Earth and at 10 AU the maximum cone or polar angle of the Sun is only ~ 2°. Thus, even a small error has a large effect on the computed orientation of the measured field relative to coordinates centered on the planet.

The magnetic field data are obtained in a quasi-inertial reference coordinate frame aligned with the ecliptic plane and are then transformed to a spherical coordinate system centered on Saturn and rotating with the planet; these data are combined with information on the spacecraft position to yield a measurement set with six variables. The adopted position of the rotation axis of Saturn is $\lambda_S = 78.81°$ and $\beta_S = 61.93°$, corresponding to ecliptic longitude and latitude in 1950.0 coordinates. The adopted rotation rate and reference meridian are those defined by the Jet Propulsion Laboratory (*3*) and correspond to a rotation period of 10 hours 14 minutes. In this coordinate system longitude increases eastward on the planet.

A total of 203 vector measurement sets were obtained during the close encounter phase on 1 September 1979, both inbound to and outbound from periapsis, corresponding to radial distances between 1.34 and 5 Saturn radii (R_S) (1 R_S = 60,000 km). During radio occultation, a reduced spacecraft data rate was in effect, so that this preliminary report includes no data from 1.34 to 2.29 R_S while outbound.

A projection of the spacecraft flyby trajectory onto the surface of the planet is shown in Fig. 1. Within 5 R_S, the latitude and longitude coverage extends only from 3.7° to −6.2° and 270° to 200°, respectively. To obtain a unique mathematical representation of the planetary field, observations over a closed surface containing the magnetic field sources are required. A flyby trajectory allows the acquisition of data only along the spacecraft path, and thus the mathematical models that can be derived from the observations are not unique. The Pioneer 11 encounter trajectory, with its limited coverage, provides a restricted sampling of the planetary field and imposes restrictions on the complexity of physically meaningful mathematical models that can be used to fit the observations. In general, this limitation is expressed in terms of the sensitivity of the problem to the propagation and amplification of errors and is quantitatively expressed by the condition number of the matrix associated with a least-squares fitting procedure (*4*).

The magnetic field, B, in a region containing no sources ($\nabla \times B = 0$) can be expressed as the gradient of a scalar potential V, which represents the contributions of sources internal and external to the region of interest. It is customary to express the potential in terms of spherical harmonics as

$$V = V^e + V^i = a \sum_{n=1}^{\infty} \{(r/a)^n T_n^e + (a/r)^{n+1} T_n^i\}$$

where r is the distance from Saturn's center, a is Saturn's radius, and the $T_n^{i,e}$ are given by

$$T_n^i = \sum_{m=0}^{n} P_n^m (\cos\theta) \times [g_n^m \cos m\phi + h_n^m \sin m\phi]$$

and

$$T_n^e = \sum_{m=0}^{n} P_n^m (\cos\theta) \times [G_n^m \cos m\phi + H_n^m \sin m\phi]$$

0036-8075/80/0125-0444$00.50/0

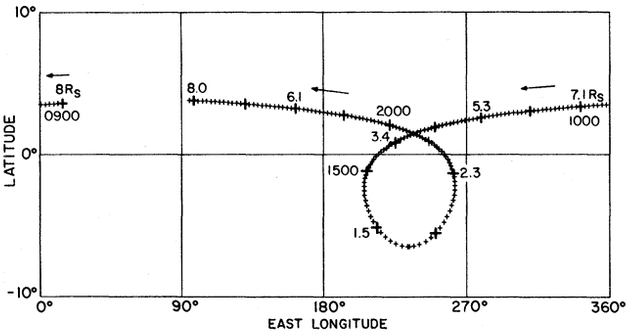

Fig. 1 (left). Subsatellite trace of Pioneer 11 trajectory on the surface of Saturn in kronographic coordinates, 1 September 1979. Time marks at hourly intervals are indicated by crosses, and a few are labeled. Fig. 2 (right). Comparison of observed (+) and modeled (solid curve) magnetic field of Saturn.

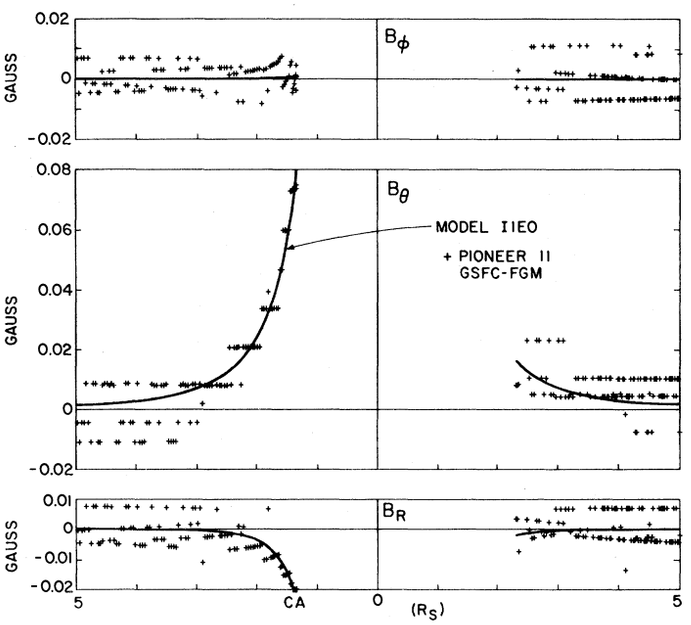

where the angles ϕ and θ denote kronographic east longitude and co-latitude, respectively. The values of $P_n^m(\theta)$ are Schmidt-normalized associated Legendre functions, and g_n^m, h_n^m, G_n^m, and H_n^m are the Schmidt coefficients.

The data obtained by the FGM experiment inside 5 R_S have been plotted in the Saturn-centered spherical coordinate system as a function of radial distance (Fig. 2). Also shown are the theoretical field components (solid lines) derived from a magnetic field model obtained by fitting the observations in a least-squares sense to a first degree ($n = 1$) spherical harmonic expansion representing sources of internal origin only, thus corresponding to a planetary-centered, but tilted, dipole. The condition number of the equation set we used is approximately 2 to 3.

The dipole moment obtained from this model is 0.20 ± 0.01 gauss-R_S^3 ($4.3 \pm 0.2 \times 10^{28}$ gauss-cm^3). The dipole is oriented in opposite polarity to that of Earth, and its tilt with respect to the rotational axis of the planet is $2° \pm 1°$. Including an external term of order $n = 1$ in the model does not significantly reduce the root-mean-square of the residuals in the least-squares fit or change the variables determined. This results in part from the quantization step size of the instrument, which is large relative to the measured field magnitude. Using data sets with smaller radial distance coverages than 5 R_S (namely to 3.5 R_S) leads to the quoted uncertainties in the dipole moment estimate. The near alignment between the dipole and rotational axes leads to a highly axisymmetrical inner magnetosphere, as evidenced by the charged particle observations (*5–8*).

The dipole moment derived above is smaller by a factor of 4 or more than was anticipated on the basis of postulated scaling laws for the generation of planetary magnetic fields and the interpretation of the reported detection of Saturn at hectometer wavelengths (*9, 10*). The assumption of a common physical mechanism for the origin of planetary magnetism has given rise to a number of scaling laws that attempt to relate the magnetism of the planets to conditions in their interiors, despite the nonlinear nature of the dynamo problem. The currently accepted mechanisms for the generation of planetary fields are either a precession- or convection-driven dynamo operating in the planet's interior. The apparent correlation between a planet's angular momentum and its dipole magnetic moment (magnetic "Bode's law") is a simple scaling relationship and has also been used to estimate the dipole moment of Saturn. This moment corresponds to a surface equatorial field strength of approximately 0.8 gauss. A slightly higher value was inferred from the radio astronomical observations by Kaiser and Stone (*10*). The model derived from the Pioneer observations yields an equatorial surface field strength of 0.2 gauss and a maximum field at the poles of 0.56 gauss when the dynamic flattening of the planet (1/10.4) has been taken into account.

The discrepancy between the predictions and observations is illustrated in Fig. 3, where the known dipole moments (or upper limits) of the planets are plotted against their angular momenta. A possible conclusion of the "abnormally low" dipole moment and highly dipolar geometry of the field is that the field generating region—the liquid core or shell where the dynamo is active—is small, as was originally expected (*11*).

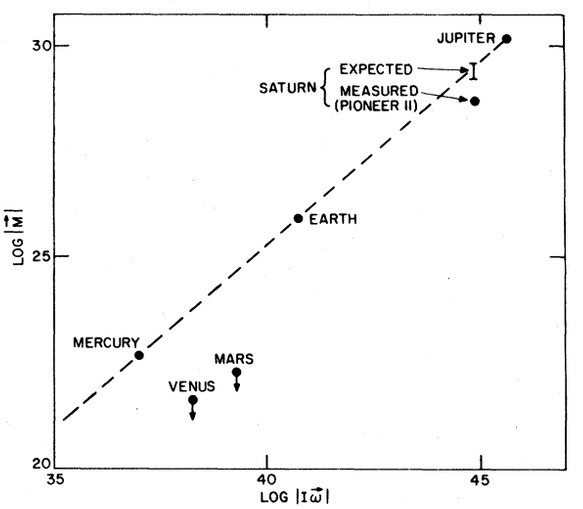

Fig. 3. Magnetic "Bode's law" showing the approximate relationship of planetary magnetic field dipolar moments versus spin angular momenta.

The derived alignment between the dipole and rotational axes constitutes a perplexing observation. On Jupiter there exists a strong longitudinal control of the probability of detecting decametric radio bursts; it is reasonable to expect, however, that this will not be the case for Saturn. Thus the lack of longitudinally varying features in the radio spectrum would parallel the observed lack of significant longitudinal features in the planet's atmosphere, as seen in the visible spectrum. Determining Saturn's rotation period with an accuracy comparable to that of Jupiter may be extremely difficult.

The axisymmetrical and dipolar field suggests that, in the inner magnetosphere, charged particle sweeping effects by satellites and particulate rings should have sharp and spatially limited boundaries when observed from a spacecraft in a flyby trajectory, as well as being extremely stable because longitudinally varying radial disturbances are absent. In addition, in an axisymmetrical dipolar field, the radial extent of the L shell regions associated with satellites or particulate rings, where particle absorption effects are observed, is determined by the physical dimensions of the satellite or ring as well as by its orbital eccentricity since the magnetic dipole axis coincides with the focal point of the orbit. This interpretation of course assumes that radial diffusion processes have a characteristic time scale that is long compared with the bounce and drift periods of energetic particles in the L shells.

Thus, a centered dipole field at the planet, aligned with the rotation axis, results in the minimum possible radial extent for the absorption regions. A more complex field, or the representation of the field as an offset tilted dipole, would result in wider absorption regions (unless of course the offset is along the dipole axis) since the range of L shells swept by the satellite or ring as the planet rotates would be increased. Thus, the observed radial extent and symmetry of sweeping effects of satellite and particulate ring impose a maximum bound on the equatorial offset, which can be physically justified in an offset, tilted dipole representation of the planetary magnetic field.

For the planetary dynamo theory, the near alignment between the magnetic and rotation axes further illustrates the apparent paradox associated with Cowling's theorem and the generation of planetary fields by the dynamo mechanism. This theorem states that an axisymmetric flow cannot generate a self-regenerative dynamo, but Braginsky (*12*) has shown that small deviations from axisymmetry can lead to dynamo-generated fields if the magnetic Reynolds number is sufficiently high. Thus, the observed near alignment at Saturn may provide an important new constraint for models of planetary dynamos. This constraint was previously unsuspected because, in all magnetic planets for which in situ observations were available before the Saturn encounter, the angle observed between the magnetic and rotational axes has typically been of the order of 10° (*13*).

The Saturn satellite Titan is among one of the most interesting "lunar" objects in the solar system because of its large size and measurable atmosphere. Conventional estimates of the strength of the planetary field combined with estimates of the solar wind momentum flux at 10 AU had indicated that Titan was always immersed deeply within the Saturnian magnetosphere, because the average distance to the magnetopause was estimated to be 40 R_S. The Pioneer 11 results, however, estimate the average position to the magnetopause to be approximately 20 R_S, equal to the orbital radius of Titan. Hence, Titan will be located within the outer magnetosphere, the magnetosheath of Saturn, or even the interplanetary medium. Titan is thus subjected for an appreciable fraction of time to the depositional-erosional effects of a subsonic or supersonic but highly thermalized solar wind. Titan's environment is expected to be much more variable than was previously anticipated. The Voyager 1 spacecraft will pass within 7000 km of Titan on 11 November 1980 at a local (Saturn) time of approximately 1400 hours. Because of the possible fluctuating character of the environment, deductions of Titan's physical properties may be much more difficult for the fields and particles experiments measuring in situ.

MARIO H. ACUÑA
NORMAN F. NESS
Laboratory for Extraterrestrial Physics, NASA/Goddard Space Flight Center, Greenbelt, Maryland 20771

References and Notes

1. M. H. Acuña and N. F. Ness, *Space Sci. Instrum.* **1**, 177 (1975).
2. E. J. Smith, *Jet Propulsion Laboratory Tech. Rep. 616-48* (1973).
3. F. Sturms, *Jet Propulsion Laboratory Rep. 32-1503* (1971).
4. M. H. Acuña and N. F. Ness, in *Magnetospheric Particles and Fields*, B. M. McCormac, Ed. (Reidel, Dordrecht, Netherlands, 1976), pp. 311–325.
5. W. Fillius, W. H. Ip, C. E. McIlwain, *Science* **207**, 425 (1980).
6. J. H. Trainor, F. B. McDonald, A. W. Schardt, *ibid.*, p. 421.
7. J. A. Simpson, T. S. Bastian, D. L. Chenette, G. A. Lentz, R. B. McKibben, K. R. Pyle, A. J. Tuzzolino, *ibid.*, p. 411.
8. J. A. Van Allen, M. F. Thomsen, B. A. Randall, R. L. Rairden, C. L. Grosskreutz, *ibid.*, p. 415.
9. F. H. Busse, in *Solar System Plasma Physics*, C. F. Kennel, L. J. Lanzerotti, E. N. Parker, Eds. (North-Holland, Amsterdam, 1979).
10. M. L. Kaiser and R. G. Stone, *Science* **189**, 285 (1975).
11. W. B. Hubbard and R. Smoluchowski, *Space Sci. Rev.* **14**, 599 (1973).
12. S. I. Braginskiy, *Geomag. Aeron.* **15**, 127 (1975).
13. N. F. Ness, *Moon Planets* **18**, 427 (1978).
14. We thank D. Stillwell and J. Lepetich for their efforts in implementing the experiment. We also thank R. Thompson, F. W. Ottens, G. Burgess and J. Connerney for their prompt analysis of these data.

3 December 1979

Vertical Structure of the Ionosphere and Upper Neutral Atmosphere of Saturn from the Pioneer Radio Occultation

Abstract. *Radio occultation measurements at S band (2.293 gigahertz) of the ionosphere and upper neutral atmosphere of Saturn were obtained during the flyby of the Pioneer 11 Saturn spacecraft on 5 September 1979. Preliminary analysis of the occultation exit data taken at a latitude of 9.5°S and a solar zenith angle of 90.6° revealed the presence of a rather thin ionosphere, having a main peak electron density of about 9.4 × 10^3 per cubic centimeter at an altitude of about 2800 above the level of a neutral number density of 10^{19} per cubic centimeter and a lower peak of about 7 × 10^3 per cubic centimeter at 2200 kilometers. Data in the neutral atmosphere were obtained to a pressure level of about 120 millibars. The temperature structure derived from these data is consistent with the results of the Pioneer 11 Saturn infrared radiometer experiment (for a helium fraction of 15 percent) and with models derived from Earth-based observations for a helium fraction by number of about 4 to 10 percent. The helium fraction will be further defined by mutual iteration with the infrared radiometer team.*

The flight path of the Pioneer Saturn spacecraft during its encounter with Saturn on 5 September 1979 is described elsewhere in this issue (*1*). Near the closest approach point of its trajectory, the spacecraft was occulted by Saturn at a distance of about 55,000 km from the occulting limb. The occultation tangency point was on the evening terminator at a latitude of about 11.5°S and a solar ze-

0036-8075/80/0125-0446$00.75/0